MEASUREMENT OF CELLULAR SECONDARY FLOW OVER A LONGITUDINALLY RIDGED BED

ZHI-QIAN WANG, NIAN-SHENG CHENG, YEE-MENG CHIEW
School of Civil and Environmental Engineering, Nanyang Technological University
Singapore 639798

Longitudinal bedforms consisting of ridges or troughs parallel to the main flow may occur in wide rivers, tide-swept seas or other deformable boundaries. Most previous investigations have been devoted to the understanding of the primary mechanism that leads to the formation of sand ridges. Longitudinal ridges are usually associated with cellular secondary flows and transverse wall stresses, which in turn can enhance or maintain the size of ridges for mobile bed conditions. In the earlier experiments conducted by the authors (Wang, et al 2003), cellular secondary flows over rough/smooth strips in a flat-bed channel were investigated. In this study, secondary flows over a longitudinally ridged bed are measured. Both LDA and UDV were used to provide 3D velocity information for the induced secondary flows. The results show that the structure of secondary flows over ridges/troughs is similar to that over rough/smooth strips. It is also suggested that the secondary flow could be assessed by considering the variation of the bed shear stress.

1 Introduction

Longitudinal bedforms are elongated in shape, with its major axis parallel to the mean flow motion, such as longitudinal desert dunes, sand ribbons on sea and river beds, and other linear forms apparently dependent on wave-action at the strand (Allen, 1984). In fluvial environment, longitudinal bedforms usually possess a smaller dimension than transverse bedforms, because they are best visible at, or close to, transition to upper plane-bed phase. Sometimes, longitudinally scoured troughs or grooves with large sizes are also observed. Longitudinal bedforms appear as periodic, spanwise variations in bed texture and/or bed elevation, and tend to be remarkably uniform in the streamwise direction. Karcz (1966) and Allen (1966) in particular made the interpretation of longitudinal sand ridges or strips in terms of secondary flows (see Fig. 1). In marine environment, sand ribbons aligned with the strongest tidal currents have been widely identified in shallow tide-swept seas (e.g. Kenyon and Stride, 1970; Karl, 1980; Stride, 1982). Marine sand ribbons typically are found on extensive level surfaces underlain by lag gravels or smoothed rock. They are spaced transversely in the order of 10-200m, and range up to 15km in length, but seldom rise more than 1m above their surroundings (Allen, 1984). Longitudinal ridges and furrows of low relief occasionally appear on continuous beds of homogeneous sand. It has been also observed that systems of longitudinal vortices are apparently developed in the ebbing tidal current at the sites of the ridges and furrows.

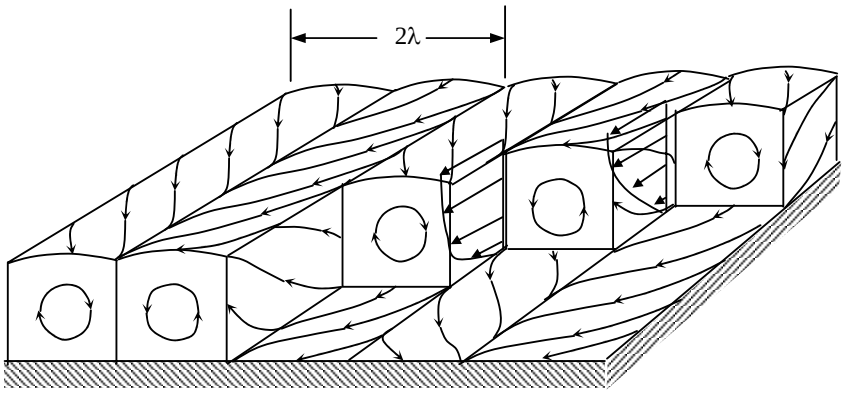

Figure 1. General structure of secondary flows in a straight channel (after Allen, 1984), where λ is half wavelength of secondary flow and corresponding bed forms.

Longitudinal bedforms can also be reproduced in laboratory experiments. Casey (1935) conducted a sediment transport experiment using mixed grades of sand in a straight flume. He noticed that the finer particles moved over the coarser in the form of longitudinal bands or ribbons which he called *Längsstreifen*. He further explained them with a secondary flow having a spanwise wavelength of roughly twice the flow depth. Similar observations were also made by Vanoni (1946), Allen (1966), Günter (1971), Ikeda (1981), Hirano and Ohmoto (1988), Nezu and Nakagawa (1989) and McLelland, et al. (1999). Relevant flow structures have been measured by Müller and Studerus (1979), Mclean (1981), Studerus (1982), Nezu and Nakagawa (1984) and Wang et al. (2003). Regardless of these previous efforts, the results obtained are still preliminary and some phenomena are not well understood.

It is noted that the bedforms concerned may either comprise alternate longitudinal rough/smooth strips or alternate ridges/troughs, or both. In the earlier research presented by the authors (Wang, et al., 2003), cellular secondary flows induced by the lateral roughness variation in a flat-bed channel were examined experimentally. This paper aims to investigate similar structures related to a longitudinally ridged bed but without roughness variations. This work serves as one of the essential components for the on-going research project to explore characteristics of open channel flow and sediment transport affected by longitudinal bedforms.

2 Experiments

The experiments were carried out in a straight rectangular tilting flume at the Hydraulics Laboratory of NTU. The flume was 14 m long, 0.6 m wide and 0.6 m deep. It had two glass sidewalls and a flat steel bottom, strengthened together by a steel framework. The slope of the flume was changeable through motor-driven adjustable jacks. The flume bed was covered by laterally corrugated metal sheets, whose cross-section is shown in Fig. 2.

The shape of the corrugated surface was assumed to represent the naturally-developed longitudinal ridges. However, lateral roughness variations were not considered. The spacing of adjacent ridges, 2λ, remained constant at 150mm, and the bed configuration was arranged to be symmetrical with a valley located at the centerline of the channel. The coordinates used in this paper are also shown in Figure 2.

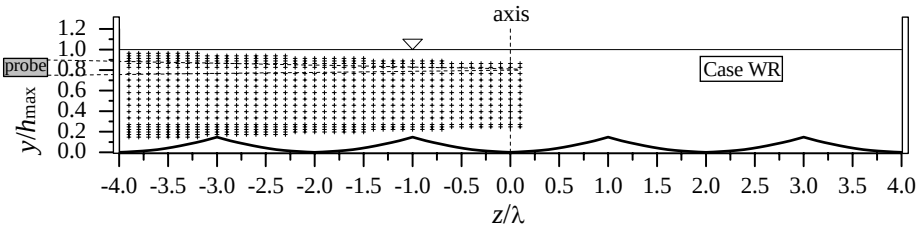

Figure 2. Cross-section of the flume (looking downstream). The wavy line at the bottom represents the longitudinal ridges and troughs. Crosses are the sampling points for LDA; LDA probe and UDV transducer were mounted normal to the sidewall.

The flow discharge was fixed at 84 m^3/h and the cross-sectional mean velocity was 0.507 m/s. The maximum flow depth over the valley was about 81mm and the minimum water depth over the ridge cusp was 69mm. The average width-to-depth ratio *(B/h)* was 8, which was large enough such that the central region of the channel was unaffected by the sidewalls.

The velocity was measured over a cross section 8-meter downstream from the inlet, where the flow was fully developed and nearly uniform. Two kinds of measurement instruments were used in the experiment: Laser Doppler Anemometry (LDA) and Ultrasonic Doppler Velocimetry (UDV). The LDA employed was a DANTEC measurement system (Flowlite 2D), which included an integrated four-beam, a two-component laser-optics unit, a signal processor, a set of application software and other accessories. It was operated in the backscatter mode with a 400mm-focal-length lens that produced a sampling volume of 0.12×0.12×2.6mm measured in the downstream (*x*), vertical (*y*), and spanwise (*z*) directions. The laser-optics unit was mounted on an automated traverse carriage. With the two-dimensional LDA, difficulties were encountered to directly measure the spanwise velocity of an open channel flow because the flume bottom was opaque. This is because the spanwise velocity can only be measured from a plane perpendicular to it, but laser beams will be disturbed by the water surface fluctuations if transmitting from the top. Thus, the LDA system was only used to detect the velocity components in the streamwise and vertical directions, for which laser beams passed through one of the sidewalls. Only half of the cross section was measured because the flow structure was expected to be symmetrical along the central line because of the symmetrical bed configuration. The sampling points are marked as crosses in Fig.2.

A UDV system, DOP2000-model 2125, was also introduced to the experiment for measuring the spanwise velocity. With pulsed Doppler ultrasound, a short ultrasonic burst was sent periodically. Then a receiver collected continuously echoes, which came from targets that were present in the path of the ultrasonic beam. By sampling the incoming echoes relative to the emission of the bursts, the shift of positions of scatterers were thus measured. The main advantage of pulsed Doppler ultrasound is its capability to offer spatial information associated with velocity values. In this study, the spanwise velocity was measured by mounting the transducer onto the external surface of the side glass wall without intrusion to the flow field. The sampling positions were at the same heights used for LDA. The spanwise velocity over the whole section was measured.

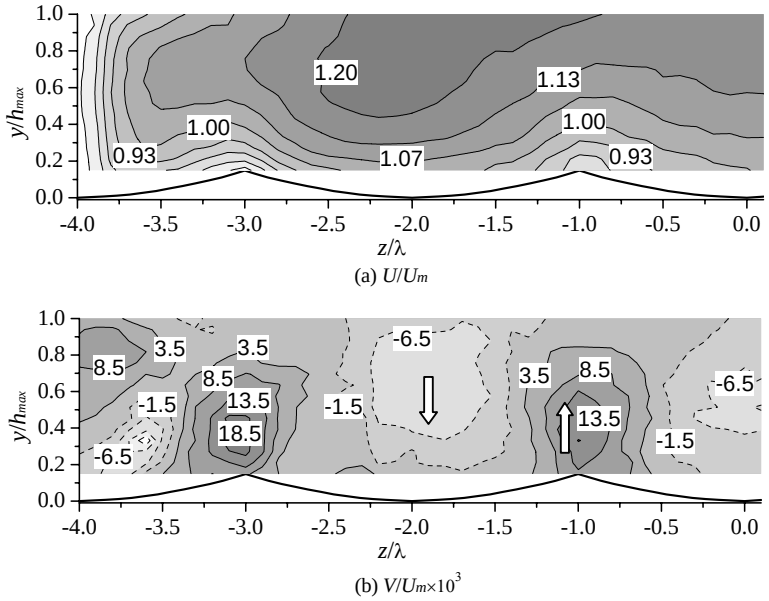

Figure 3. Contour plots of (a) dimensionless mean streamwise velocity (U/U_m); and (b) dimensionless mean vertical velocity ($V/U_m \times 10^3$).

3 Data Analysis and Results

Fig. 3(a) shows the contour map of the mean streamwise velocity. It is noted that sidewall effects are dominant in the region nearly two times the water depth from the side wall. This could be roughly judged from the phenomenon of 'velocity dip', i.e. highest velocity at each vertical line appearing below the water surface. In the central region, the bed configuration dominates the flow pattern. The contour of the streamwise velocity varies approximately according to the bottom shapes; the streamwise velocity above the ridges is less than that above the troughs at the same elevation.

Fig. 3(b) shows the vertical velocity contours. Downflow occurs over the troughs while upflow over the ridges. This flow pattern is similar to that observed over the flat-bed channel with the rough/smooth strips, in which upflow occurs over the smooth strips and downflow over the rough strips (Wang et al., 2003). The upflow is more concentrated around the ridge cusps and has a greater magnitude than that of the downflow. The maximum magnitude of the upflow velocity occurs nearly at $0.4y/h_{max}$, while that for the downflow at $0.6y/h_{max}$. The periodical distribution of upflow and downflow signifies the existence of secondary flow cells.

Fig. 4 plots the spanwise velocities measured using the UDV at 15 different elevations. Near the sidewalls, the acoustic field was modified, which resulted in considerable noises. The badly affected regions are denoted by circles in Fig. 4, and the central region was free from such influence. Fig. 4 demonstrates that the spanwise velocity fluctuates in a sinusoidal form. This fluctuation is consistent with the wavelength of ridges. The positive velocity indicates the left-to-right motion, while the negative value indicates the right-to-left motion. At the lower portion of the flow, the transverse motion is directed from the valleys to the ridge cusps, while at the upper portion, the transverse motion occurs in the opposite direction.

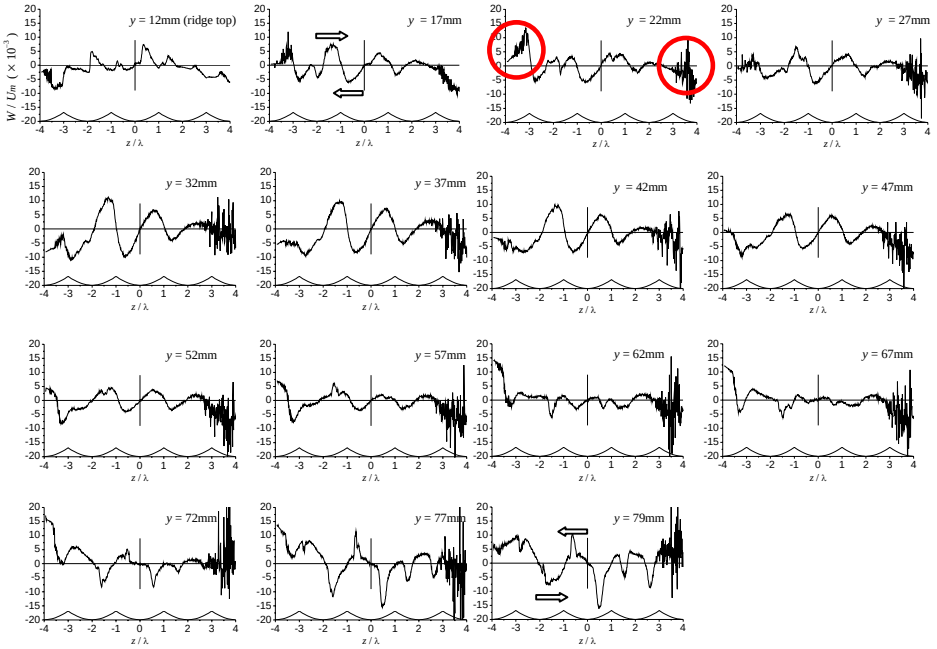

Figure 4. Transverse profiles of spanwise velocity at 15 elevations, which measure from the lowest point of trough. The circles denote the region where noise is dominant due to the glass-water interface influence.

Using the measured V (from LDA) and W (from UDV), a plot of cross-sectional velocity vectors can be obtained. Fig. 5 shows the counter-rotating secondary flow cells

that occur over the cross section; they separate over the ridge cusps or the valley bottoms. These flow cells have a width of half ridge spacing and a height of water depth. The mean magnitude of the velocity vectors shown in Fig. 5 is $0.007U_m$ and the largest magnitude is $0.022U_m$. From the organized secondary flow structures, one may conjecture a clear picture of the sediment transport over the ridged bed.

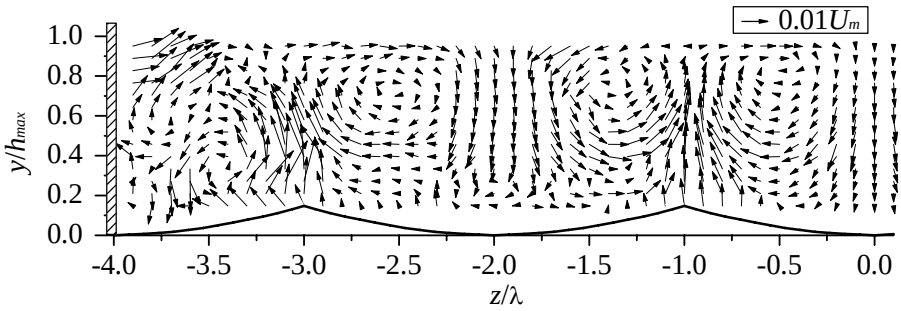

Figure 5. Velocity vectors on the cross section.

4 Discussion

This study demonstrates that the longitudinal ridges with the wavy section are also able to induce cellular secondary motions in an open channel flow. The observed secondary flow pattern is very similar to that over flat beds with rough/smooth strips (Müller and Studerus, 1979; Wang et al. 2003). This similarity suggests that the secondary flow could be initiated with the lateral perturbation in bed shear stress τ_b, which could be caused by the lateral variations either in bed elevation or in bed roughness. This bed perturbation will further induce lateral gradient of the Reynolds stresses in the whole flow field so that streamwise vortices that characterize the secondary flow will be finally developed.

From the above consideration, we may assume that the intensity of cellular secondary flows can be assessed simply using the amplitude of the bed shear stress variation. The latter can be taken as $\Delta\tau_b = \max(\tau_b)-\min(\tau_b)$. For the case of the wavy channel bed, if the variation in the bed elevation is small, $\Delta\tau_b$ can be approximated as

$$\Delta\tau_b \propto \gamma J\left[\max(b)-\min(b)\right] \tag{1}$$

where γ = specific gravity of fluid; J = slope of the flow; and b = local bed elevation measured from the lowest point of the bed.

Because of the symmetrical bed configuration, the bed shear stress would distribute in a sinusoidal fashion in the spanwise direction. Given the lateral coordinate with z = 0 being located at the channel centerline, a cosine term can be used to describe the shear stress fluctuation. Therefore, τ_b can be expressed as

$$\tau_b = \gamma JH + a\gamma J\left[\max(b) - \min(b)\right]\cos(k_b \frac{z}{2\lambda}) \quad (2)$$

where H = average flow depth; k_b = wave number; and a = coefficient. The first term on the right hand side of Eq. (2) is the average bed shear stress. Some analyses have been conducted to formulate vertical distributions of the Reynolds shear stress with the boundary condition given by Eq. (2) but the results are not shown here due to the limited space.

5 Conclusions

Secondary flows in open channel were generated in this study using the longitudinally ridged bed. Flow measurements were conducted in the three directions using LDA together with UDV. The experimental results show that the secondary flow consists of circulation cells with the downflow appearing over the troughs and the upflow over the ridges. The lateral and vertical dimensions of the circulation away from the sidewall are approximately equal, being close to the flow depth. The flow structure over the ridges is very similar to that over rough/smooth strips. The intensity of the secondary flow might be assessed by considering the perturbation of the bed shear stress, which is simply related to the bed elevation perturbation for the present case.

References

Allen J.R.L. (1984). *Sedimentary Structure, Sedimentary: their character and physical basis.* Elsevier, Amsterdam, The Netherlands, Vol. II.

Allen, J.R.L. (1966). "On bedforms and palaeocurrents." *Sedimentology*, 6: 153-190.

Casey, H.J. (1935). *Mitt. Preussische Versuchsanst*. Wasserbau Schifbau, 1.

Günter, A. (1971). "Die kritische mittlere Sohlenschubspannung bei Geschiebemischungen unter Berücksichtigung der Deckschichtbildung und der turbulenzbedingten Sohlenschubspannungsschwankungen." *Mitteilung der Versuchsanstaltfür Wasserbau an der ETH Zurich*, Vol. 3.

Hirano, M. and Ohmoto, T. (1988). "Experimental study on the interaction of between longitudinal vortices and sand ribbons." *Proceedings of 6th Congress of APD-IAHR*, Vol. II: 59-65.

Ikeda, S. (1981). "Self-formed straight channels in sandy bed." *Journal of Hydraulic Division*, ASCE, 107: 389-406

Karcz, I. (1966). "Secondary currents and the configuration of a natural stream bed." *Journal of Geophysical Research*, 71: 3109-3116.

Karl, H.A. (1980). "Speculation on processes responsible for mesoscale current lineations on the continental shelf, southern, California." *Marine Geology*, 34: M9-M18.

Kenyon, N.H. and Stride, A.H. (1970). "The tide-swept continental shelf sediment between the Shetland Isles and France." *Sedimentology*, 14: 159-173.

Mclean, S.R. (1981). "The role of non-uniform roughness in the formation of sand ribbons." *Marine Geology*, 42: 49-74.

McLelland, S.J., Ashworth, P.J., Best, J.L. and Livesey, J.R. (1999). "Turbulence and secondary flow over sediment strips in weakly bimodal bed material." *Journal of Hydraulic Engineering*, ASCE, 125(5): 463-473.

Müller, A. and Studerus, X. (1979). "Secondary flow in an open channel." *Proceedings of 18th IAHR Congress, Cagliari*, vol.3: 19-24.

Nezu, I. and Nakagawa, H. (1984). “Cellular secondary currents in straight conduit.” *Journal of Hydraulic Engineering*, ASCE, 110: 173-193.

Nezu, I. and Nakagawa, H. (1989). “Self forming mechanism of longitudinal sand ridges and troughs in fluvial open channel flows.” *Proceedings of 23rd IAHR Congress*, Ottawa, Canada, B56-B72.

Nezu, I. and Nakagawa, H. (1993). *Turbulence in open channels*. Balkema, Rotterdam, The Netherlands.

Stride, A.H. (1982). *Offshore Tidal Sands*, Processes and Deposits, Chapman and Hall, London.

Studerus, X. (1982). “Sekundärströmungen im offenen Gerinne über rauhen Längsstreifen.” Ph.D. Thesis, Institut für Hydromechanik und Wasserwirtschaft, ETH, Zürich, Switzerland.

Vanoni, V.A. (1946). “Transportation of suspended sediment by water.” *Transactions of ASCE*, 111: 67-133.

Wang, Z.Q., Cheng, N.S., Chiew, Y.M., and Chen, X.w. (2003). “Secondary flows in open channel with smooth and rough bed stripes.” *Proceedings of 30th IAHR Congress*, Thessaloniki, Greece, Theme C, Vol. 1: 111-118.